Tribology Letters, Vol. 18, No. 3, March 2005 (© 2005)
DOI: 10.1007/s11249-004-2757-4

An extension of the Hertz theory for three-dimensional coated bodies

S.B. Liu[a], A. Peyronnel[b], Q.J. Wang[a,*] and L.M. Keer[a]

[a]*Department of Mechanical Engineering, Northwestern University, Evanston, IL 60208, USA*
[b]*Département de Mécanique, Ecole Polytechnique, 91128 Palaiseau, France*

Received 26 September 2004; accepted 31 October 2004

This paper presents a work on extending the Hertz theory for circular and elliptical point contact problems involving coated bodies. The extended form of the Hertzian formulae are adopted to express maximum contact pressure, contact radius, and contact approach in terms of applied load, equivalent radius, and an extended equivalent modulus that properly considers the presence of a coating. The extended equivalent modulus is a function of Young's moduli and Poisson's ratios of the coating and the substrate, coating thickness, and a parameter, which is obtained through substantial numerical simulation. The extended Hertzian formulae are easy to use and give accurate predictions of contact characteristics.

KEY WORDS: contact mechanics, Hertz theory, coating, equivalent Young's modulus

Nomenclature

W	applied force
R, R_1, R_2	radius
E_1, E_2, E_c, E_s	Young's modulus
E_i^*	equivalent modulus; $E_i^* = \frac{E_i}{1-\nu_i^2}$
E^*	total equivalent modulus
E	modulus ratio; $E = E_c^*/E_s^*$
ν_1, ν_2, ν_c, ν_s	Poisson's ratio
r_a, r_b, a	contact semi-axes and contact radius
r_{a0}, r_{b0}, a_0	contact radius determined by the Hertz theory
p_0	maximum contact pressure determined by the Hertz theory
δ_0	contact approach or rigid body motion
h	coating thickness
H	non-dimensional thickness; equation (7)
μ	Shear modulus ratio
τ	dimensionless thickness; h/a
α	parameter
subscript: 1, 2	identifying body
subscript: c, s	identifying coating and substrate
$\bar{a}, \bar{\delta}, \bar{p}, \bar{r}_a, \bar{r}_b$	dimensionless variables normalized by values from the Hertz theory
ζ	semi-axes ratio; $r_{b0}/\ r_{a0}$

1. Introduction

Since the seminal paper published by Hertz in 1882 [1], contact mechanics has become one of the important fields in engineering mechanics. Contact theories can be found in various application; for example, with the development of instrumented indentation methods, materials can be quantitatively characterized using contact probe techniques. Research publications on contact problems are widely distributed among technical journals; however, there are also several excellent books available, among them are those by Galin (1953), Gladwell (1980), Johnson (1985) and Goryacheva (1998). In the following, the three-dimensional (3D) Hertz theory is described and studies on contact problems for coated bodies are briefly reviewed.

1.1. 3D Hertz theory for circular point contacts

Figure 1(a) presents two frictionless, elastic, isotropic, and homogeneous convex solids of revolution ($R_{1x} = R_{1y} = R_1$ and $R_{2x} = R_{2y} = R_2$), which are brought into contact under an applied load, W. Each of the bodies has Young's modulus, E_i, and Poisson's ratio, ν_i, where the subscript refers to the respective body. If the size of the contact area is small compared to the size of both solids, the contact problem in figure 1(a) is equivalent to one between a half-space and a virtual solid with equivalent radii ($R_x = R_y = R$, $R^{-1} = {R_1}^{-1} + {R_2}^{-1}$), as shown in figure 1(b), where the virtual solid can be treated as a rigid body. The classic Hertz theory [2] gives, in a concise and unique form, a set of exact contact formulae for the contact approach, pressure distribution, and contact radii. These formulae [2] are convenient to use and have been widely applied in both academic modeling and engineering practice,

*To whom correspondence should be addressed.
E-mail: qwang@northwestern.edu

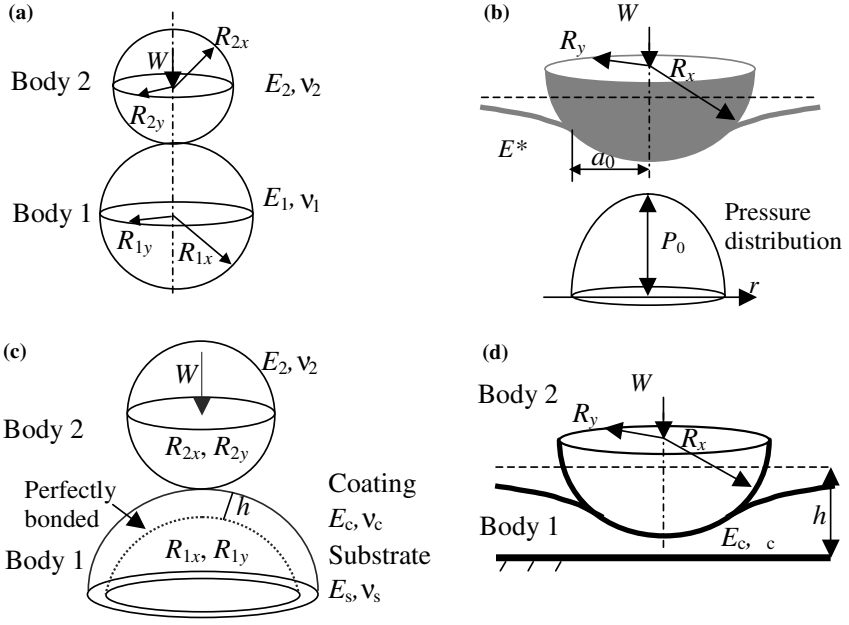

Figure 1. Problem description: (a) Hertzian contact; (b) equivalent Hertzian contact; (c) contact with a coated body; (d) contact with a rigid substrate.

- contact radius, a_0:$a_0 = \sqrt[3]{\dfrac{3WR}{4E^*}}$ (1a)

- contact approach or rigid body motion, δ_0:

$$\delta_0 = \sqrt[3]{\frac{9W^2}{16RE^{*2}}} \tag{1b}$$

- maximum contact pressure, p_0:

$$p_0 = \sqrt[3]{\frac{6WE^{*2}}{\pi^3 R^2}} \tag{1c}$$

- pressure distribution, p_d:

$$p_d = p_0\sqrt{1-(r/a_0)^2} \tag{1d}$$

where R is the equivalent radius, $\mathrm{R}^{-1} = \mathrm{R_1}^{-1} + \mathrm{R_2}^{-1}$, E^* the total equivalent modulus,

$$\frac{1}{E^*} = \frac{1-\nu_1^2}{E_1} + \frac{1-\nu_2^2}{E_2} \tag{2}$$

and $E_i^* = \frac{E_i}{1-\nu_i^2}$ the equivalent modulus. The characteristic of addition between the inverse values of equivalent moduli offers the convenience of a single variable for various material combinations.

1.2. 3D Hertz theory for elliptical point contacts

The elliptical point contact applies to two frictionless, elastic, isotropic, and homogeneous ellipsoids or cylinders in contact having principal radii of curvature of their surface at the origin, R_{ix} and $R_{iy}, i = 1$ or 2 (figure 1(a)). The principal relative radii of curvature are denoted by R_x (major) and R_y (minor) ($R_x > R_y$) and the angle between their axes for each surface is denoted by θ. Their relationships are expressed as follows,

$$R_x^{-1} + R_y^{-1} = R_{1x}^{-1} + R_{1y}^{-1} + R_{2x}^{-1} + R_{2y}^{-1} \tag{3a}$$

$$(R_y^{-1} - R_x^{-1})^2 = (R_{1x}^{-1} - R_{1y}^{-1})^2 + (R_{2x}^{-1} - R_{2y}^{-1})^2 + 2(R_{1x}^{-1} - R_{1y}^{-1})(R_{2x}^{-1} - R_{2y}^{-1})\cos(2\theta) \tag{3b}$$

The equivalent radius of curvature can be defined as $R = \sqrt{R_x R_y}$. Assuming that the elliptic contact region has semi-axes r_{a0} (major) and r_{b0} (minor), they are related to the principal relative radii of curvature in terms of their ratio, $\zeta = r_{b0}/r_{a0}$,

$$\frac{R_x}{R_y} = \frac{\mathbf{E}(e)/\zeta^2 - \mathbf{K}(e)}{\mathbf{K}(e) - \mathbf{E}(e)} \tag{4}$$

where $e = \sqrt{1-\zeta^2}$ and $\mathbf{K}(e)$ and $\mathbf{E}(e)$ are complete elliptical integrals of the first and second kind. Equation (4) could be used to find the ratio, ζ. The contact characteristics between the two bodies are complicated and include complete elliptical integrals as follows,

• semi-axes, r_{a0} and r_{b0} :

$$r_{a0} = F_0(e)\sqrt[3]{\frac{3WR}{4E^*}} \quad \text{and} \quad r_{b0} = r_{a0}\,\zeta \tag{5a}$$

• equivalent contact radius, $a_0 = \sqrt{r_{a0} r_{b0}}$:

$$a_0 = F_1(e)\sqrt[3]{\frac{3WR}{4E^*}} \tag{5b}$$

• contact approach, or rigid body motion, δ_0:

$$\delta_0 = F_2(e)\sqrt[3]{\frac{9W^2}{16RE^{*2}}} \tag{5c}$$

• maximum contact pressure, p_0:

$$p_0 = \frac{1}{[F_1(e)]^2}\sqrt[3]{\frac{6WE^{*2}}{\pi^3 R^2}} \tag{5d}$$

• pressure distribution, p_d:

$$p_d = p_0\sqrt{1-(x/r_{a0})^2-(y/r_{b0})^2} \tag{5e}$$

where

$$[F_0(e)]^3 = \frac{4}{\pi\, e^2}\sqrt{[\mathbf{E}(e)/\zeta^2 - \mathbf{K}(e)][\mathbf{K}(e) - \mathbf{E}(e)]} \tag{6a}$$

$$F_1(e) = F_0(e)\sqrt{\zeta} \tag{6b}$$

$$F_2(e) = \frac{2}{\pi}\sqrt{\zeta}\frac{\mathbf{K}(e)}{F_1(e)} \tag{6c}$$

The other parameters are the same as in cases with solids of revolution mentioned for circular point contacts. It is clear that these results consist of the Hertzian relationship of spherical contact and several functions of the semi-axis ratio. Figure 4.4 in [2] shows the results of ζ, $F_1(e)$, and $F_2(e)$ in terms of the ratio, R_x/R_y, for easy and efficient evaluation. Johnson [2] further pointed out that even for $\zeta = 1/3$, using equations (1) and the equivalent radius $R = \sqrt{R_x R_y}$ leads to overestimating a_0 and δ_0 by only 5% and to underestimating p_0 by 8%.

1.3. Studies on coating problems

Coatings with a uniform thickness, h, can be used for surface strengthening, friction and wear control, and corrosion prevention. However, the Hertz theory is not applicable for analyzing the contact behavior between coated bodies. Figure 1(c) shows a coating perfectly bonded (bonded case) to a substrate. The material properties of the coating and the substrate are identified with subscript "c" and "s", respectively. It is convenient to make the coating thickness a non-dimensional variable. The Hertzian solutions between body 1 with the substrate alone and body 2 are denoted by δ_{0s}, a_{0s}, and p_{0s}. On the other hand, if the coating is infinitely thick, the corresponding Hertzian solutions are denoted by δ_{0c}, a_{0c}, and p_{0c}. The non-dimensional coating thickness is defined as

$$H = h/a_{0s} \tag{7a}$$

for elastic substrates and

$$H = h/a_{0c} \tag{7b}$$

for rigid substrates.

The case with a rigid substrate was investigated extensively with various mathematical techniques in literature, for example, by Vorovich and Ustinov [3], Keer [4], Matthewson [5], Jaffar [6], Sakamoto *et al.* [7], among many others. The counterpart is usually rigid and has a spherical or parabolic shape (figure 1(d)). Another dimensionless thickness, $\tau = h/a$, where a is the contact radius, is also used. Quantities δ_{0c}, a_{0c}, and p_{0c} are used to non-dimensionalize the contact approach (δ), contact radius (a), and maximum contact pressure (p), i.e., $\bar{\delta} = \delta/\delta_{0c}$, $\bar{a} = a/a_{0c}$, and $\bar{p} = p/p_{0c}$. Vorovich and Ustinov [3] found approximate solutions in a form of infinite series for a thick ($h/a > 1.5$) layer bonded to a rigid substrate in contact with a rigid parabolic body,

$$\bar{\delta} = 1 - 0.504H^{-1} - 0.225H^{-3} - 0.098H^{-5} - 0.197H^{-6} + \cdots \tag{8a}$$

$$\bar{a} = 1 - 0.113H^{-3} + 0.114H^{-5} + 0.025H^{-6} - 0.004H^{-7} + \cdots \tag{8b}$$

$$\bar{p} = 1 + 0.225H^{-3} - 0.018H^{-5} - 0.0126H^{-6} + 0.013H^{-7} + \cdots \tag{8c}$$

When the indenter is elastic, Keer [4] derived the contact solutions by analogy with the method used in [3] and by introducing the ratio of elastic properties into the solution. El-Sherbiney and Halling [8] and Wang and Lakes [9] also studied this problem. The expressions for contact radius and approach between the elastic indenter and the thick ($h/a > 1.5$) layer bonded to the rigid substrate are given by [4] (see also [8]),

$$\bar{\delta} = 1 - 0.504 C_E H^{-1} - C_E^2 (0.225 H^{-3} + 0.098 H^{-5} + \cdots) + \cdots \tag{9a}$$

$$\bar{a} = 1 + C_E (-0.113 H^{-3} + 0.114 H^{-5} + 0.025 C_E H^{-6} + \cdots) \tag{9b}$$

where C_E is the equivalent modulus ratio, $C_E = E_2^*/(E_c^* + E_2^*)$ (figure 1(d)). Matthewson [5] studied axi-symmetric indentation problems with rigid indenters, such as spheres and cones, pressed into a thin ($h/a < 1/2$) layer bonded to a rigid substrate. Analytical expressions were derived and substantiated by experiments. For the incompressible thin layer of $v_c = 1/2$ on a rigid substrate in contact with a rigid spherical indenter, Matthewson found the following relationship between load and contact radius, a,

$$W = \frac{\pi E_c a^3}{16(1+v_c)R\tau}\left[9 + \frac{1}{4\tau^2} + \frac{3}{2\tau^2(2+c)}\right] \tag{10}$$

or

$$(\bar{a})^{-3} = \frac{3\pi(1-v_c)}{64\tau}\left[9 + \frac{1}{4\tau^2} + \frac{3}{2\tau^2(2+c)}\right]$$

where $c = \frac{xK_0(x)}{K_1(x)}$ is evaluated at $x = \frac{\sqrt{6}}{3\tau}$, and K_0 and K_1 are the zero-order and first-order modified Bessel functions. Jaffar [6] derived asymptotic expressions for pressure distribution and contact radius of thin ($h/a < 0.1$) elastic layered bonded and unbonded to a rigid substrate. Sakamoto *et al.* [7] assumed that contact pressure was the summation of Tchebycheff polynomials (equation (10) in [7]) with unknown coefficients. Both bonded and unbonded layers were considered, which were in contact with either spherical or flat-ended cylindrical indenters. The effect of the thickness and Poisson's ratio of an elastic layer on the parameter, $W/(2E_c^* a\delta)$ or $2/(3\bar{a}\bar{\delta})$, was depicted in figure 2 [7].

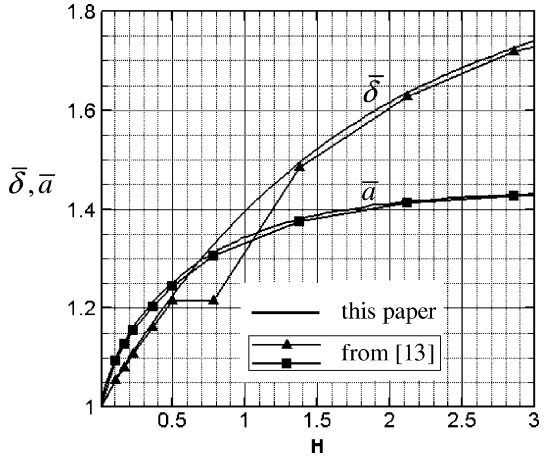

Figure 2. Comparison with results from Chen and Engel [13].

El-Sherbiney and Halling [8] proposed correction factors in the form of a decreasing function of $H = h/a_{0c}$, to take into consideration the elasticity of the substrate. Surprisingly, the substrate properties do not influence the two factors. Keer *et al.* [10] constructed a model to analyze the effects of normal and tangential loading on two identical, coated, elastic spheres. The model however is limited to $h/a > 0.2$. Eberhardt and Keer [11] introduced an additional middle layer with the same material properties of the substrate in order to enhance convergence for problems with thin (e.g. h/a is as small as 0.05) layers. Ogilvy [12] presented a curve-fitted expression based on the approximate results obtained by El-Sherbiney and Halling [8]. It should be noted that different interpretations from the original definitions are questionably applied to film thickness and reduced modulus ratio. By using the numerical model of Chen and Engel [13], Stevanovic *et al.* [14] presented approximate models for predicting the contact radius between a sphere and a layered body. When the substrate is rigid, the following relationship is obtained by curve-fitting,

$$\bar{a} \equiv a/a_{0c} = 1 - 1.04\ \exp(-1.73\tau^{0.734}) \tag{11}$$

For elastic substrates, the following approximate solution for the contact radius were also obtained,

$$\bar{a} \equiv a/a_{0s} = 1 + (\gamma - 1)\left\{1 - \exp\left[-\gamma^{\pi/8}\ \sqrt[4]{\pi(H/d)^{\pi}}\right]\right\} \tag{12}$$

where

$$d = 1 + (\gamma - 1)\left\{1 - \exp\left[-\gamma^{\pi/8}\ \sqrt[4]{\pi[2H/(1+\gamma)]^{\pi}}\right]\right\}$$

and $\gamma = a_{0c}/a_{0s}$.

It is noticed that existing asymptotic or approximate expressions are only applicable to rigid substrates, and numerical results for elastic substrates are available only for cases with specified material properties. This work extends the Hertz theory to solve the contact problems between coated components over a wide range of material properties. Numerical analyses with a computer code similar to that reported in [15] are conducted to determine a parameter involved in the expression of the extended Hertz theory. For two-dimensional cases, one can refer to the work reported in an earlier paper [16].

2. Extended Hertz theory

A frequency response function (FRF) is the counterpart in the frequency domain of a Green's function. The FRF of the surface normal displacement due to pressure on the surface of a 3-D body is expressed as follows [17],

$$\tilde{\tilde{u}} = \frac{2}{E_c^* w} \frac{1 + 4whk\vartheta - \lambda\kappa\vartheta^2}{1 - (\lambda + \kappa + 4\kappa w^2 h^2)\vartheta + \lambda\kappa\vartheta^2} \tag{13}$$

where

$$\lambda = 1 - \frac{4(1 - v_c)}{1 + \mu(3 - 4v_s)}, \quad \kappa = \frac{\mu - 1}{\mu + (3 - 4v_c)},$$
$$\vartheta = \exp(-2wh), \quad \text{and} \quad \mu = \frac{E_c(1 + v_s)}{E_s(1 + v_c)}.$$

The double tilde means two-dimensional Fourier transform with respect to x and y, and w is defined in the frequency domain and is the counterpart of radius in the space domain. μ is the shear modulus ratio and constants λ and κ in the above equation are similar to the Dundurs parameters defined for two-material composite problems. Two limiting situations can be obtained immediately:

$$\text{(a)} \quad \tilde{\tilde{u}} = \frac{2}{E_s^* w} \tag{14}$$

for zero H (i.e., no coating). In the derivation, the following identity is used

$$\frac{1 - \lambda\kappa}{1 - (\lambda + \kappa) + \lambda\kappa} = \frac{E_c^*}{E_s^*},$$

and

$$\text{(b)} \quad \tilde{\tilde{u}} = \frac{2}{E_c^* w} \tag{15}$$

for infinite H (i.e., no substrate). Since the coating has different material properties from the substrate, the mechanical responses of a coated half-plane are due to the combined contribution of the coating and substrate materials. These responses can be regarded as arising from another equivalent half-space with mingled properties. By comparing the form of equations (13) and (15), a new equivalent modulus is defined as follows:

$$E_1^* = E_c^* \frac{1 - (\lambda + \kappa + 4\kappa w^2 h^2)\theta + \lambda\kappa\theta^2}{1 + 4whk\theta - \lambda\kappa\theta^2} \tag{16}$$

where w now denotes a different variable. After defining $\alpha = wh/H$, the above modulus is a function of material properties (μ_c, μ_s, v_c, v_s), coating thickness (H), and the parameter (α),

$$E_1^* = E_c^* \frac{1 - (\lambda + \kappa + 4\kappa\alpha^2 H^2)\exp(-2\alpha H) + \lambda\kappa\exp(-4\alpha H)}{1 + 4\alpha H\kappa\exp(-2\alpha H) - \lambda\kappa\exp(-4\alpha H)} \tag{17}$$

For the contact between an equivalent half-space (as body 1) and another half- space (as body 2), the equivalent Young's modulus in equation (2) becomes

$$\frac{1}{E^*} = \frac{1}{E_1^*} + \frac{1 - v_2^2}{E_2} \tag{18}$$

This treatment can be applied to body 2 in the same way, if it is also a coated body. In order to obtain better agreement, the parameter of α and thus E_1^* have different values for the contact approach, contact radius, and maximum contact pressure. The value of α can be obtained by comparing the numerical results and the predictions from using equations (1) or (5) with equations (17) and (18) instead of equation (2). The predicted quantities or contact characteristics obtained from equations (1) or (5) are denoted by the same names but without subscript "0", which is for homogeneous body only. The process to determine α for all characteristics is discussed in Sections 3 and 4 for circular point contact with elastic and rigid substrates, respectively. In Section 5, the extended Hertz theory is used to predict characteristics for elliptical point contact.

3. Elastic substrate cases in circular point contact

Elastic substrates are discussed first, since they represent a more realistic tribology application than rigid substrates. In this case, numerical simulations require a substantial amount of code development, and a certain amount of computation time has to be used to determine contact performance. In the numerical analysis, contact constraints have to be satisfied through an iteration scheme. The discrete convolution and fast Fourier transform (DC-FFT) algorithm [18] is applied to improve the simulation efficiency. Quantities a_{0s}, p_{0s}, and δ_{0s} are used to non-dimensionalize the contact radius (a_{num}), maximum contact pressure (p_{num}), and contact approach (δ_{num}) determined with the simulation code, i.e., $\bar{a} = a_{\text{num}}/a_{0s}$, $\bar{p} = p_{\text{num}}/p_{0s}$, and $\bar{\delta} = \delta_{\text{num}}/\delta_{0s}$. Note that the non-dimensional coating thickness is defined in equation (7a) with a_{0s} as well. The computation domain is divided into 128×128 grids. It is found that the contact radius determined from contact area S, $a_{\text{num}} = \sqrt{S/\pi}$, is less sensitive to discretization. In order to verify our code, Chen and Engel's results with $E = 1/3$ and both Poisson's ratios as 1/3 (table 2 in [13]) are converted into $\bar{a}$ and $\bar{\delta}$ by algebraic calculation and plotted in figure 2 in terms

of H. Our results with the same E but slightly different Poisson's ratios of 0.3 are shown for comparison. The agreement is satisfactory except at one data point. By checking figure 8—a graphical form of table 2 in the same paper [13], this discrepancy is due to a typo.

The indenter is assumed to be rigid to simplify the determination of α. If the indenter is elastic, its contribution to contact behavior can be determined by including the equivalent modulus in E^* of equation (2). The relationship between α and Poisson's ratio is not clear at the beginning, so the Poisson's ratios for both bodies are first assumed to be 0.3. It is noted that contact characteristics, such as in Chen and Engel's results [13], depend on the modulus ratio, $E = E_c^*/E_s^*$, but not on their absolute values. Therefore in the analyses, E or E_c^*/E_s^* varies from 0.25 to 4 and has 25 values in total: $1/E = 4 - (i-1)/4$, $i = 1 \ldots 12$ and $E = 1 + i/4$, $i = 0 \ldots 12$. The value for H has a range of 0.01–3 and 101 values in total. These 2525 results of non-dimensional $\bar{a}$, $\bar{p}$, and $\bar{\delta}$ with different modulus ratio are shown in figure 3, plotted against the non-dimensional coating thickness. It is obvious that when H is reduced, all curves approach unity. On the other hand, when H is sufficiently large, each curve approaches a constant predicted by the Hertz theory, i.e., $\bar{a} = E^{-1/3}$, $\bar{p} = E^{2/3}$, and $\bar{\delta} = E^{-2/3}$. It is also noted that coated components with $E_c^* E_s^*$ behave differently from those with $E_c^* < E_s^*$, particularly in terms of the maximum contact pressure. Comparing to results in 2D cases [16], figures 3 (a) and (b) have similar trend of variation for $\bar{a}$ and $\bar{p}$ but with different magnitudes.

It is not difficult to see that with appropriate α values, equations (1) with (17) and (18) can predict the contact approach, contact radius, and maximum contact pressure accurately. However, α values depend on H and E_c^*/E_s^* in a complicated way as shown in figure 4, where α_a, α_p, and α_δ are α values for $\bar{a}$, $\bar{p}$, and $\bar{\delta}$, respectively. One can argue that curves with $E_c^* > E_s^*$ share one trend and curves with $E_c^* < E_s^*$ have the other. A few representative curves of α, instead of all

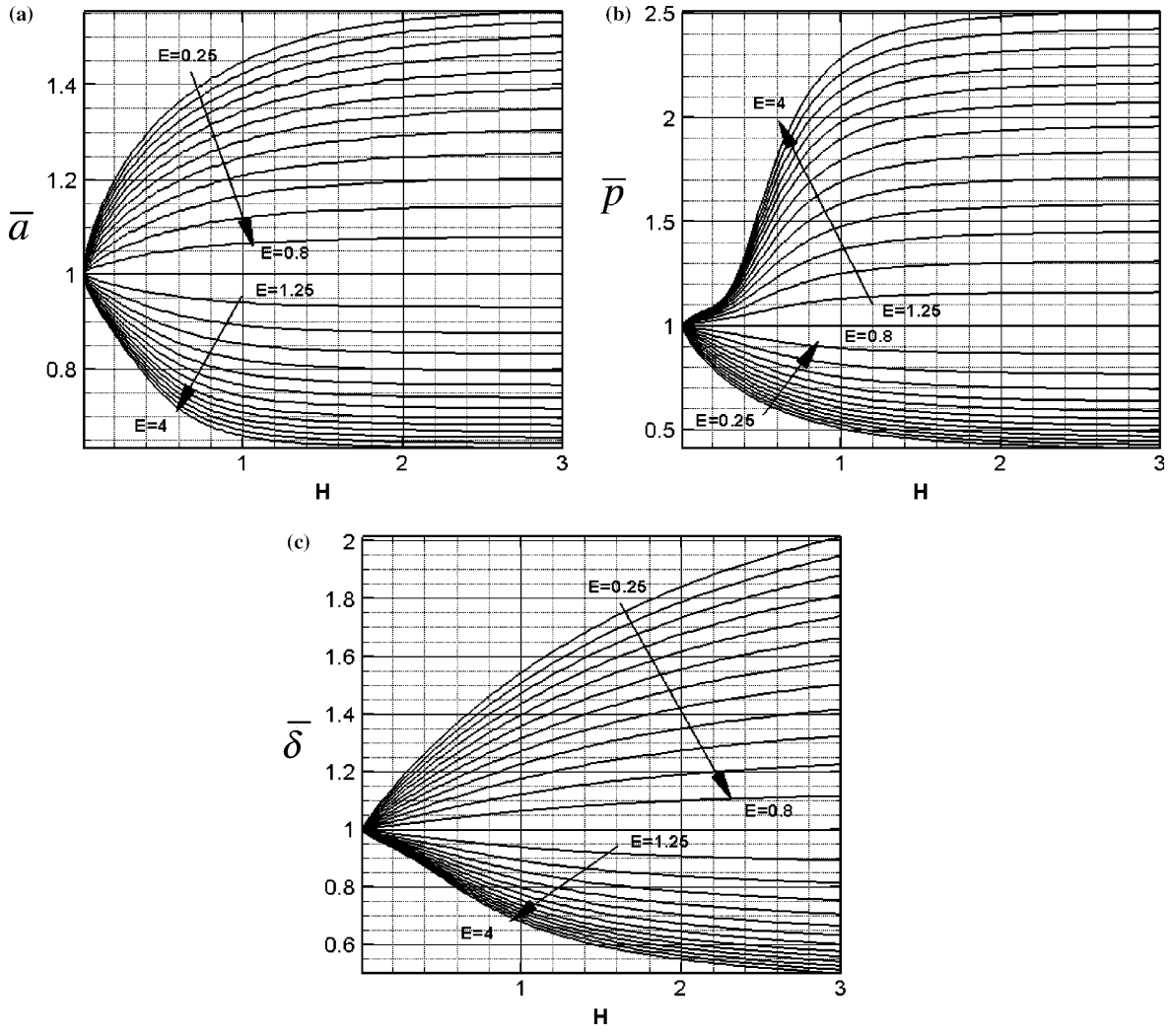

Figure 3. Contact characteristics: (a) $\bar{a}$; (b) $\bar{p}$; and (c) $\bar{\delta}$ with different modulus ratio against non-dimensional coating thickness (H).

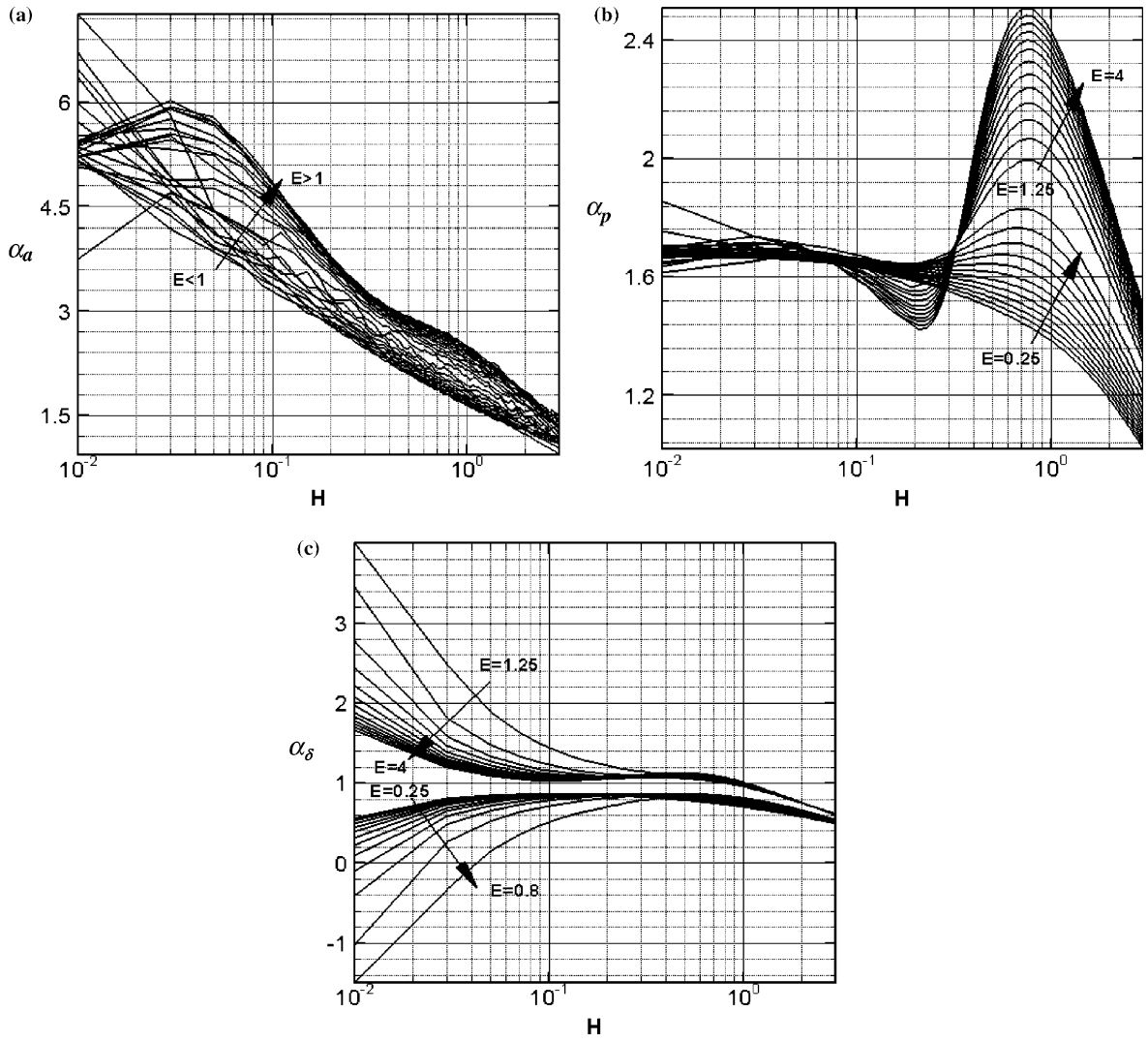

Figure 4. Values of the parameter (α) against H with different modulus ratio E: (a) $\bar{a}$; (b) $\bar{p}$; and (c) $\bar{\delta}$.

curves, may be chosen for convenience. Six curves are selected with modulus ratio of 1/3 and 3, denoted as $\alpha_a(1/3)$ and $\alpha_a(3)$ for contact radius; $\alpha_p(1/3)$ and $\alpha_p(3)$ for maximum contact pressure; and α_δ (1/3) and α_δ (3) for contact approach. These curves are shown in figure 5. Values of α for other modulus ratios are expressed in terms of modulus ratio (E) as follows,

$$\alpha_p(E) = \begin{cases} \alpha_p(1/3) - (1/E - 3)/14 & E \in [1/4,\ 1/3] \\ 1.85 + [\alpha_p(1/3) - 1.85]/(3E) & E \in [1/3,\ 1] \\ 1.72 + E[\alpha_p(3) - 1.72]/3 & E \in [1,\ 3] \\ \alpha_p(3) - (E - 3)/25 & E \in [3,\ 4] \end{cases} \tag{19a}$$

$$\alpha_\delta(E) = \begin{cases} \alpha_\delta(1/3) - (1/E - 3)/39 & E \in [1/4,\ 1/3] \\ 0.685 + [\alpha_\delta(1/3) - 0.685]/(3E) & E \in [1/3,\ 1] \end{cases} \tag{19b}$$

Error used to quantify the accuracy of prediction is defined as the difference in percentage between the values predicted with equations (1) and (17–19) and the numerical solutions normalized by the latter. It is

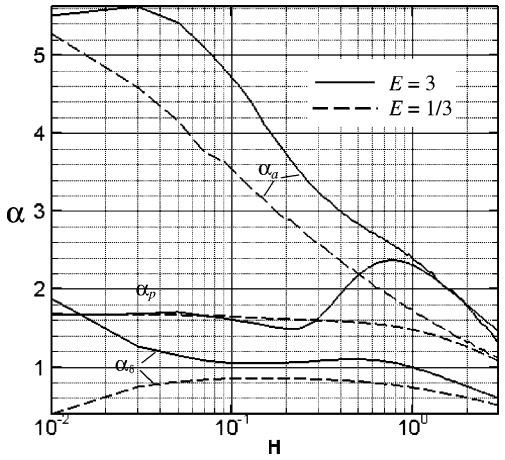

Figure 5. Representative values for the parameter (α) against H.

found that for all cases analyzed in figure 3, the absolute values of error are less than 1.5%.

In real applications, Poisson's ratio may differ from 0.3, e.g., about 0.2 for grey cast iron. Examinations are conducted with Poisson's ratio of the substrate fixed at 0.3 and that of the coating varying from 0.15 to 0.3, i.e., $0.15 + (i-1) \times 0.3$, $i = 1,\ldots,6$. These examination cases also have four different modulus ratios: 4, 1.25, 0.8, 0.25. Here, 2424 cases are studied to check error. For $E = 0.25$ and $v_c = 0.15$, the absolute values of error are large for some values of H, but less than three percent. Therefore, the parameter, α, defined in equation (19) is reasonable for prediction of circular point contact characteristics.

Stevanovic *et al.* [14] defined the following dimensionless contact radius and coating thickness,

$$a^* = \frac{a_{num} - a_{0s}}{a_{0c} - a_{0s}} \tag{20a}$$

$$\tau^* = \sqrt[3]{\frac{h}{a_{num}}\sqrt{\frac{a_{0c}}{a_{0s}}}} \tag{20b}$$

and reported that the numerical results of contact radius of a 3D contact problem between an elastic sphere and a coated half-space fall on a single curve. Figure 3(a) is transformed into figure 6 of a^* against τ^*. One can arguably claim that all curves fall into a single curve, particularly in the region of τ^* from 0.8 to 1.4. However, It is found that all curves with $E_c^* > E_s^*$ are close to each other, so are all curves with $E_c^* < E_s^*$, which follow a slightly different path. The authors checked the accuracy of the approximate solution of equation (12) proposed by Stevanovic *et al.* [14] with regard to our numerical results in figure 3(a) or figure 6, and found that equation (12) has error in the range of [0, 8] and [−2.5, 0] for $E_c^* > E_s^*$ and $E_c^* < E_s^*$, respectively.

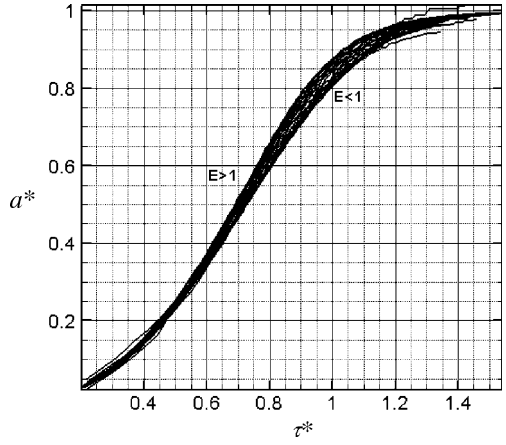

Figure 6. Variable a* against τ* (elastic substrate).

4. Rigid substrates cases in circular point contact

When the substrate is rigid (figure 1(d)), equation (17) is still valid and the two constants are $\lambda = 4v_c - 3$ and $\kappa = 1/\lambda$. In this case, quantities δ_{0c}, a_{0c}, and p_{0c} are used to non-dimensionalize δ, a, and p. Vorovich and Ustinov [3] obtained approximate solutions, equation (8) in Section 1, for contact characteristics for thick layers ($\tau > 1.5$). Matthewson [5] derived a simple solution, equation (10), for contact radius for thin layers ($\tau < 0.5$), when the layer is incompressible. Recently, Stevanovic *et al.* [14] proposed a simple expression, equation (11), for contact radius with any value of layer thickness. Figure 7 shows our numerical results of contact radius with three different Poisson's ratio (0.3, 0.4, and 0.5) against τ along with these three approximations: equation (8b) with $v_c = 0.5$ marked by triangle; equation (10) marked by rounded square; and equation (11) marked by diamond. It is obvious that our numerical results with $v_c = 0.5$ agree with both Vorovich and Ustinov's and Matthewson's work in their range of validity, and in the range of interest the curve predicted by Stevanovic *et al.* is not accurate. The comparison also suggests that Matthewson's solution can not provide accurate prediction for $\tau > 0.2$. It should be pointed out that Poisson's ratio has a significant effect on curves in figure 7, particularly when it is larger than 0.3. Figure 8 shows thirteen numerical results of contact characteristics against H from the contact simulation with $v_c = 0.3$, $E_c \in [50, 800\ \text{GPa}]$, and $E_s > 10^4\ E_c$. All results are independent of E_c and neatly fall into a single curve. When the coating thickness decreases, one can see that the maximum contact pressure increases dramati-

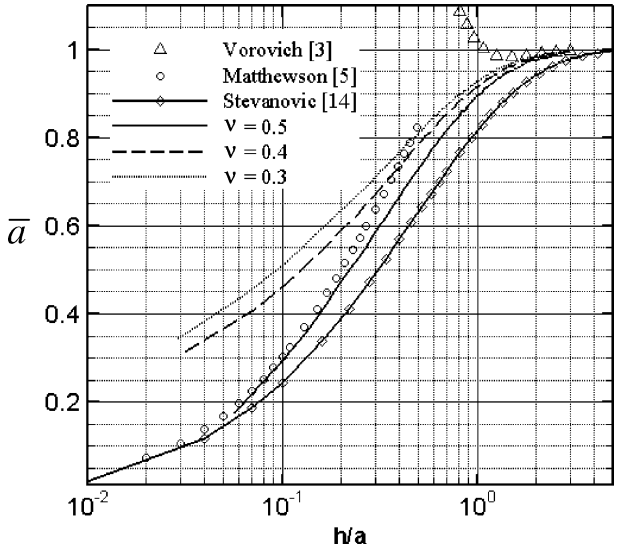

Figure 7. Comparison of results for contact radius from different work (rigid substrate).

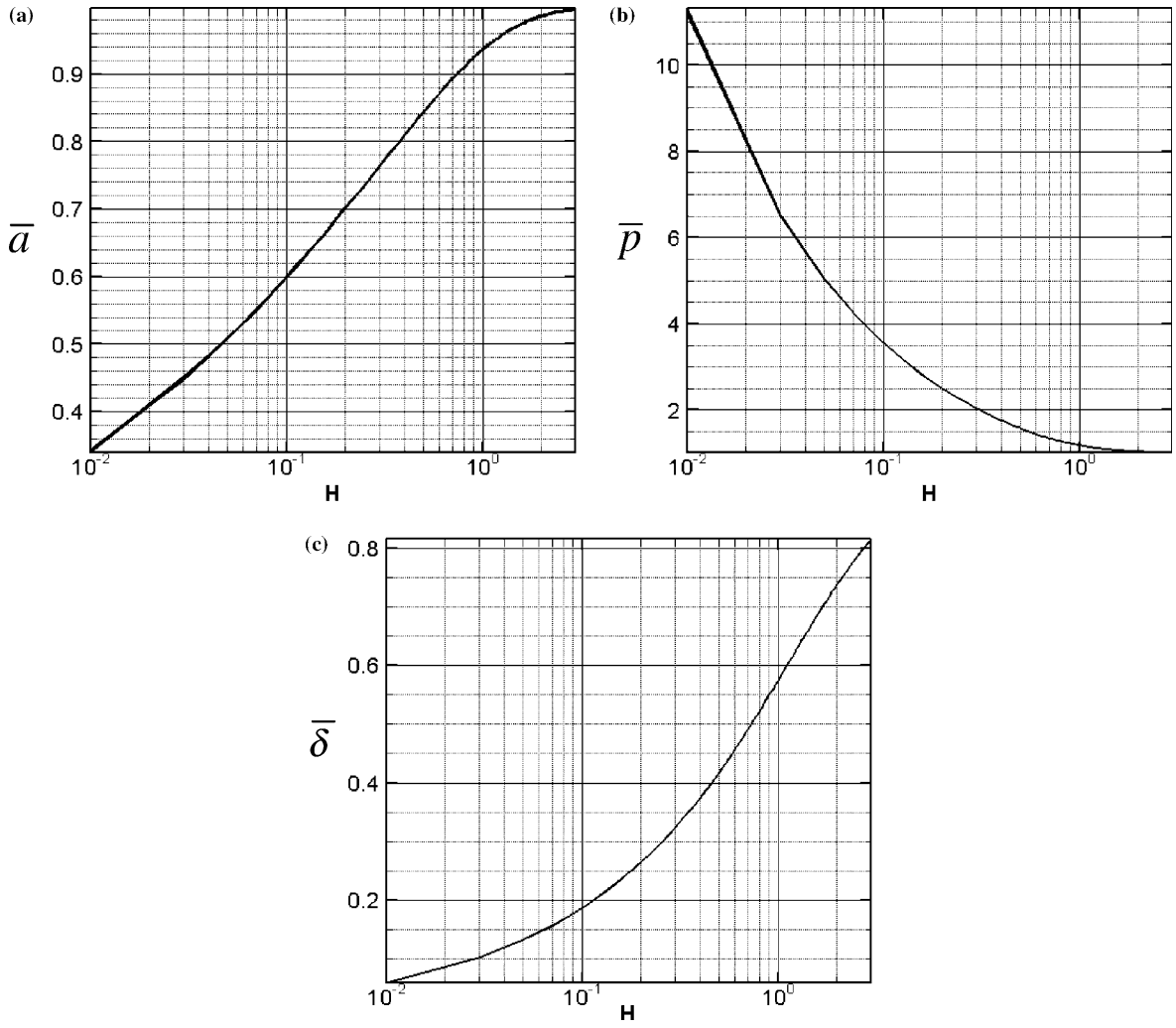

Figure 8. Contact characteristics against H (rigid substrate): (a) $\bar{a}$; (b) $\bar{p}$; and (c) $\bar{\delta}$.

cally and contact approach and radius decreases significantly. However, all curves approach unity as H increases. Similar to the case with elastic substrates, parameter α should be determined based on the numerical results. The representative α curve against H, shown in figure 9, corresponds to steel coatings ($E_c = 200$GPa, $v_c = 0.3$). When this α curve and equations (1) and (17–18) are used to predict contact characteristics of other coating materials, the absolute value of error is less than one percent.

5. Elliptical point contact

Numerical results for various layer thickness and modulus ratios were obtained for an elliptical point contact with principle radii of curvature $R' = 17.4$ mm and $R'' = 3$ mm, and load $W = 400$ N, corresponding to the example on page 97 in [2]. The ratio of the major to minor axis ($1/\zeta$) is around 3.18. In this case, the discretization interval in the minor axis direction is set as one-third of that in the major axis direction to reduce the discretization error in the

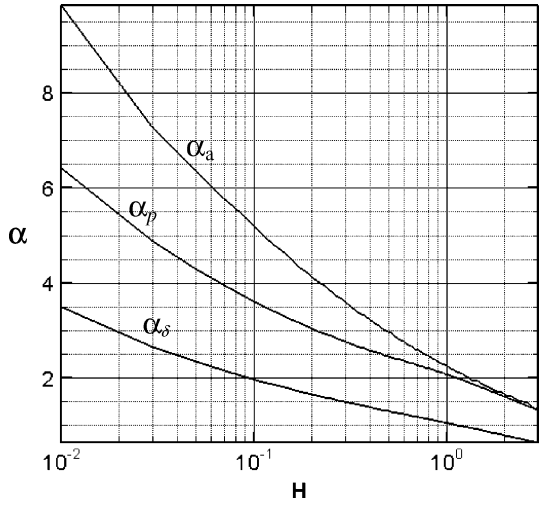

Figure 9. Representative curve against H (rigid substrate).

minor axis direction. The computation domain is divided into 128 by 128 grids. Poisson's ratio is 0.3 for the substrate and the coating. According to the error studied in Section 3, predictions for cases with modulus ratios that differ significantly from representative ones (1/3 and 3 in this paper) have slightly large error. Four cases with modulus ratios of 1/4, 0.8, 1.25, and 4 were simulated in our study. Quantities a_{0s}, p_{0s}, and δ_{0s} evaluated with equations (5b–d) are used to non-dimensionalize coating thickness and contact characteristics. The subscript 's' means that in equations (5b–d), E^* is determined by Equation (2) with no coating. The numerical results in this dimensionless form are shown in figure 10 for the major and minor semi-axes, contact approach, and maximum contact pressure. The representative α values in figure 5 for circular point contact problems are adopted here and the following expressions are used to modify α values for different E ratios:

$$\begin{cases} E \in [1/4,\ 1/3], \alpha_i(E) = \alpha_i(1/3) + (1/E - 3)/C_{1i} \\ E \in [1/3,\ 1], \alpha_i(E) = C_{2i} + [\alpha_i(1/3) - C_{2i}]/(3E) \\ E \in [1,\ 3], \alpha_i(E) = C_{3i} + E[\alpha_i(3) - C_{3i}]/3 \\ E \in [3,\ 4], \alpha_i(E) = \alpha_i(3) + (E - 3)/C_{4i} \text{ and} \\ \alpha_\delta(E) = 0.225 + E[\alpha_\delta(3) - 0.225]/3 \end{cases} \quad (21)$$

where subscript $i = a,\ b,\ \delta$, and p, and constants $C_{j\ i} = [C_{ja},\ C_{jb},\ C_{j\delta},\ C_{jp}]$ are

$$C_{ji} = \begin{bmatrix} -2.2 & 0.7 & -64 & 12 \\ 3.5 & 8.685 & 0.0885 & 2.1 \\ 0.585 & 4.685 & 0.655 & 2.65 \\ 39 & 2.92 & - & 0.926 \end{bmatrix}$$

Equations (5), (17), (18), and (21) are used to determine the prediction of contact characteristics with the α values from figure 5, and yield less than 4% overall absolute value of error for cases shown in figure 10.

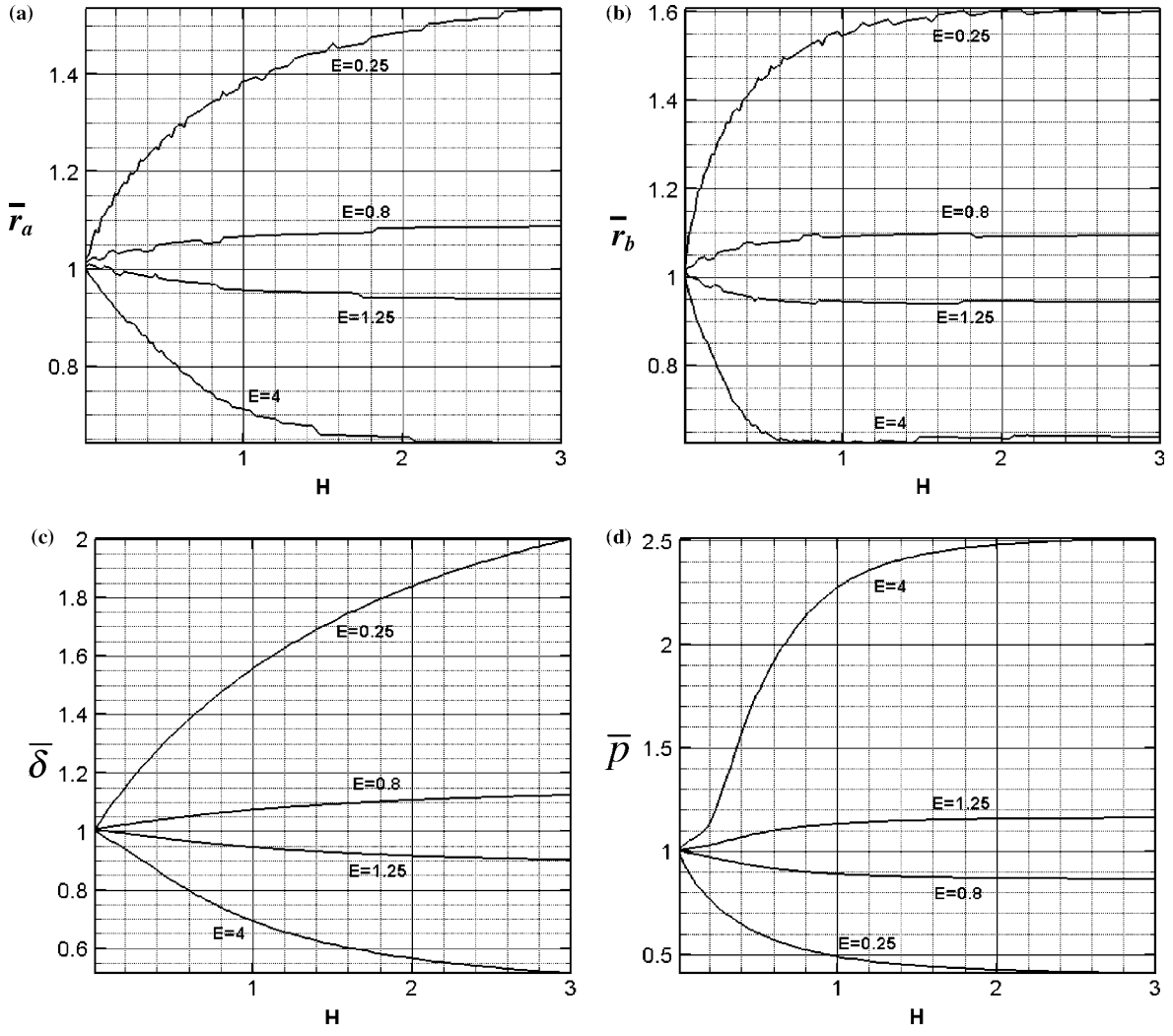

Figure 10. Elliptical point contact characteristics against H (elastic substrate): (a) major semi-axis; (b) minor semi-axis; (c) contact approach; (d) maximum contact pressure.

6. Examples

The steps of calculation using the extended Hertzian theory are illustrated in this section. Suppose a 40-μm thick boron carbide (B_4C) coating is deposited on a 52100 steel disk. Their material properties are found as following: $E_c = 380$ GPa, $v_c = 0.17$, $E_s = 200$ GPa and $v_s = 0.3$ with the modulus ratio, $E = 1.78$. Suppose further that this coated disk is loaded against a ball in a ball-on-disk test. The ball is made of 52100 steel as well and its radius is 10 mm. The applied load is 1 N. Under these conditions,

- Equation (1) gives, $\delta_0 = 0.16700$ μm, $a_0 = 40.866$ μm and $p_0 = 285.89$ MPa.
- With $h = 40$ μm, the dimensionless thickness (H) is 0.98.
- Due to $E > 1$, α curves in figure 5 for $E = 3$ are used to find $\alpha(3)$ value: $\alpha_\delta(3) \approx 1.1$, $\alpha_a(3) \approx 3.35$ and $\alpha_p(3) \approx 1.55$. After substitution of these values into equation (19), one can obtain $\alpha_\delta(1.78) \approx 1.1$, $\alpha_a(1.78) \approx 3.35$ and $\alpha_p(1.78) \approx 1.619$.
- Equation (17) gives E_1^* of 278.83, 383.22 and 319.45 GPa for approach, contact radius and maximum contact pressure, respectively. The corresponding E^* in equation (18) are 122.90, 139.68 and 130.20 GPa.
- Therefore, the approach, contact radius and maximum contact pressure are predicted by equation (1) to be 0.15500 μm, 37.727 μm and 320.12 MPa.

By comparing to the results of a numerical analysis with the contact solver: $\delta_{\text{num}} = 0.15669$ μm, $a_{\text{num}} = 38.232$ μm and $p_{\text{num}} = 325.66$ MPa, the error of the above predictions is less than 1.7%.

It is of interest to see how well the extended Hertz theory can in predict contact characteristics between two coated balls. The second example is from Keer *et al.* [10], where two coated balls are identical and have a radius of 10 mm. With the elastic properties from [10]: $E_c = 406.25$ GPa, $v_c = 0.3$, $E_s = 200$ GPa and $v_s = 0.28$, the modulus ratio is: $E = 2.06$. The applied load is 1 N. Under these conditions, equation (1) gives, $\delta_0 = 0.16842$ μm, $a_0 = 41.039$ μm and $p_0 = 283.49$ MPa. Two thickness values are studied as follows:

Case A: The thickness of the coating is 12.336 μm, and thus $H = 0.3$. Since $\alpha_\delta(3) \approx 1.1$, $\alpha_a(3) \approx 3.2$ and $\alpha_p(3) \approx 1.6$, one can obtain with equation (19) $\alpha_\delta(2.06) \approx 1.1$, $\alpha_a(2.06) \approx 3.2$ and $\alpha_p(2.06) \approx 1.638$. Equation (17) gives E_1^* of 240.94, 296.75 and 252.93 GPa for δ, a and p, which should be used for both terms in equation (18). Thus the corresponding E^* from equation (18) are 120.47, 148.38 and 126.46 GPa for δ, a and p. Finally, δ, a and p are predicted by equation (1): 0.15708 μm, 36.974 μm and 313.96 MPa. Comparing to the results of a numerical analysis with the contact solver for δ, a and p: 0.15729 μm, 37.010 μm and 314.87 MPa, the error of the above predictions is less than 0.3%.

Case B: If a thicker coating, $h = 54.648$ μm, is considered, one has $H = 1.33$. $\alpha(3)$ values are $\alpha_\delta(3) \approx 0.9$, $\alpha_a(3) \approx 2.1$ and $\alpha_p(3) \approx 2.1$, and by equation (19), one can obtain $\alpha_\delta(2.06) \approx 0.9$, $\alpha_a(2.06) \approx 2.1$ and $\alpha_p(2.06) \approx 1.98$. Equation (17) gives E_1^* of 321.38, 426.94 and 422.15 GPa for δ, a and p. Similarly to case A, the corresponding E^* from equation (18) are 160.69, 213.47 and 211.08 GPa. Therefore, the δ, a and p are predicted by equation (1): 0.12963 μm, 32.708 μm and 441.77 MPa. Comparing to the results of a numerical analysis with the contact solver for δ, a and p: 0.12984 μm, 32.828 μm and 442.46 MPa, the error of the above predictions is less than 0.4%.

These results are also in good agreement with the results published by Keer *et al.* [10] for the same problem. a/H in their notation are 3.0 and 0.6 for case A and B, respectively, in their table 2. With proper algebra, their results read $\delta = 0.15818$ μm, $a = 37.007$ μm and $p = 313.77$ MPa for case A; and $\delta = 0.13084$ μm, $a = 32.798$ μm and $p = 441.15$ MPa for case B.

7. Conclusions

This paper presents the expression for an equivalent modulus and an extension of the Hertz theory in order to predict contact approach, contact radius, and maximum contact pressure for circular and elliptical point contact problems involving coated bodies. Following the form of an analytically known frequency response function, the extended equivalent modulus due to the presence of a coating is a function of Young's moduli and Poisson's ratios of the coating and the substrate, the coating thickness, and a parameter, α. This parameter is determined based on numerical results. Representative curves of α are chosen and plotted against dimensionless coating thickness in graphs. The value of α for a specific case can be calculated using a value from these representative curves and simple relationships. For a wide range of Young's modulus and Poisson's ratio, the extended Hertz theory can provide accurate and convenient predictions.

Acknowledgments

The authors would like to express their sincere gratitude to the support from US Office of Naval Research and National Science Foundation. A.P. would also like to thank Dr. Maitournam and the Center for Surface Engineering and Tribology for his internship.

Appendix A: Curve-Fitted Expressions

Curve-fitted expressions for representative α curves shown in figure 5 are obtained as follows:

$$\alpha_a(3) = \begin{cases} 5.51, \quad H \in [0.01,\ 0.05] \\ -34.22H^3+43.67H^2-20.316H+6.331, \\ H \in (0.05,\ 0.5] \\ 0.157H^2-1.08H+3.32, \quad H \in (0.5,\ 1.5] \\ -0.5H+2.8, \quad H \in (1.5,\ 3] \end{cases}$$

$$\alpha_\delta(3) = \begin{cases} -0.252\ln H+0.389, \quad H \in [0.01,\ 0.05] \\ -49.446H^3+28.492H^2-5.106H+1.330, \\ H \in (0.05,\ 0.25] \\ -0.683H^2+0.637H+0.948, \quad H \in (0.25,\ 0.5] \\ -0.287H^2+0.211H+1.064, \quad H \in (0.5,\ 0.9] \\ 0.0466H^2-0.382H+1.328, \quad H \in (0.9,\ 3] \end{cases}$$

$$\alpha_p(3) = \begin{cases} 1.047H+1.654, \quad H \in [0.01,\ 0.05] \\ 34.734H^3-8.256H^2-1.163H+1.776, \\ H \in (0.05,\ 0.33] \\ 3.661H^3-10.456H^2+9.482H-0.410, \\ H \in (0.33,\ 0.75] \\ -0.648H^2+0.882H+2.073, \quad H \in (0.75,\ 1.2] \\ 0.0854H^2-0.779H+3.02, \quad H \in (1.2,\ 3] \end{cases}$$

$$\alpha_a(\frac{1}{3}) = \begin{cases} 197.97H^2-40.013H+5.624, \quad H \in [0.01,\ 0.1] \\ 1.853H^{-0.28}, \quad H \in (0.1,\ 0.3] \\ 1.7H^{-0.352}, \quad H \in (0.3,\ 3] \end{cases}$$

$$\alpha_\delta(\frac{1}{3}) = \begin{cases} 568.758H^3-136.497H^2+11.37H+0.518, \\ H \in [0.01,\ 0.1] \\ -0.772H^2+0.242H+0.836, \quad H \in (0.1,\ 0.3] \\ 0.0175H^2-0.183H+0.899, \quad H \in (0.3,\ 3] \end{cases}$$

$$\alpha_p(\frac{1}{3}) = \begin{cases} 0.0122H^2-0.342H+1.68, \quad H \in [0.01,\ 0.2] \\ -0.0428H^2-0.116H+1.637, \quad H \in (0.2,\ 1] \\ 0.0187H^2-0.279H+1.734, \quad H \in (1,\ 3] \end{cases}$$

Similarly, curve-fitted expressions for representative α curves shown in figure 9 are obtained as follows:

$$\alpha_a = \begin{cases} -1.725\ln H+1.21, \quad H \in [0.01,\ 0.1] \\ 2.371H^{-0.339}, \quad H \in (0.1,\ 0.5] \\ 2.228H^{-0.438}, \quad H \in (0.5,\ 3] \end{cases}$$

$$\alpha_p = \begin{cases} 2.036H^{-0.243}, \quad H \in [0.01,\ 0.5] \\ 0.115H^2-0.836H+2.805, \quad H \in (0.5,\ 3] \end{cases}$$

$$\alpha_\delta = \begin{cases} 1.039H^{-0.256}, \quad H \in [0.01,\ 0.5] \\ 0.0796H^2-0.522H+1.503, \quad H \in (0.5,\ 3] \end{cases}$$

Note that some expressions at $H = 0.01$ gives different values of α than figure 5 or 9.This is tolerable since it hardly changes the predictions.

References

[1] H. Hertz, J. reine angewandte Mathematik 92 (1882) 156.
[2] K.L. Johnson, *Contact Mechanics* (Cambridge University Press, 1985).
[3] I.I. Vorovich and I.A. Ustinov, PMM 23 (1959) 637.
[4] L.M. Keer, J. Appl. Mech. (1964) 143.
[5] M.J. Matthewson, J. Mech. Phys. Solids 29 (1981) 89.
[6] M.J. Jaffar, Int. J. Mech. Sci. 31 (1989) 229.
[7] M. Sakamoto, G. Li, T. Hara and E.Y.S. Chao, J. Biomech. 29 (1996) 679.
[8] M.G.D. El-Sherbiney and J. Halling, Wear 40 (1976) 325.
[9] Y. Wang and R. Lakes, Int. J. Solids Struct. 39 (2002) 4825.
[10] L.M. Keer, S.H. Kim, A.W. Eberhardt and V. Vithoontien, Int. J. Solids Struct. 27 (1990) 681.
[11] A.W. Eberhardt and L.M. Keer, *Advances in Engineering Tribology*, eds. Y.W. Chung and H.S. Cheng, STLE SP-31 (1991) p. 110.
[12] J.A. Ogilvy, J. Phys. D: Appl. Phys. 26 (1993) 2123.
[13] W.T. Chen and P.A. Engel, Int. J. Solids Struct. 8 (1972) 1257.
[14] M. Stevanovic, M.M. Yovanovich and J.R. Culham, IEEE Trans. Comp. Packaging Technol. 24 (2001) 207.
[15] S.B. Liu and Q. Wang, ASME J. Tribol. 123 (2001) 17.
[16] S.B. Liu, A. Peyronnel, Q. Wang and L.M. Keer, submitted to *Tribology Letters*.
[17] T. Nogi and T. Kato, ASME J. Tribol. 119 (1997) 493.
[18] S.B. Liu, Q. Wang and G. Liu, Wear 243 (2000) 101.